**(Preprint) AAS 19-657**

# SOLAR RADIATION PRESSURE EFFECTS ON THE ORBITAL MOTION AT SEL2 FOR THE JAMES WEBB SPACE TELESCOPE

**Arianda Farres [*], Jeremy Petersen[†]**

Due to James Webb Space Telescope's large sunshield, which will always be facing the Sun to protect the observatory's instruments, Solar Radiation Pressure (SRP) has an important effect on its orbital motion around SEL2. Moreover, SRP is highly dependent on the observatory's attitude with respect to the Sun-observatory line. This paper explores the impact of SRP for different attitude profiles on the size of a reference orbit.

## INTRODUCTION

The James Webb Space Telescope (JWST) is a NASA flagship mission scheduled to launch in 2021, which will be the scientific successor for the Hubble Space Telescope and the Spitzer Space Telescope. It will be launched on an Ariane 5 rocket from French Guiana on a direct injection orbit out to the Sun-Earth L2 (SEL2) point. A series of mid-course correction (MCC) maneuvers will be performed to inject the additional amount of energy required to place the observatory into a periodic orbit about SEL2. Trajectories near the collinear libration points are inherently unstable, hence periodic station-keeping maneuvers are required to maintain JWST in orbit.

The JWST mission will focus on the infrared spectrum to detect red-shifted light from the early stages of the universe, which will fill a gap in the current range of astrophysical observations and allows the exploration of a whole new set of fundamental scientific questions. To detect those faint heat signals, the observatory itself must be kept extremely cold. To protect the observatory from external sources of light and heat (like Sun, Earth, and Moon) as well as from heat emitted by the observatory itself, JWST has a 5-layer sunshield that acts like a parasol, providing shade. This sunshield will always be between the Sun/Earth/Moon and the observatory, limiting JWST's admissible set of attitudes. The sunshield is know to be highly reflective and will always be facing towards the Sun, hence Solar Radiation Pressure (SRP) plays an important roll on the observatory's dynamics.

The simplest way to account for SRP is utilizing the cannonball model, where this acceleration is directed along the Sun-spacecraft line and has a constant magnitude which depends on the spacecraft's area-to-mass ratio. However this model does not account for variation on the SRP acceleration due to changes on JWST's attitude. To accurately model the SRP for JWST, accounting for its shape and attitude, the Flight Dynamics Team (FDT) uses a polynomial curve fit provided by the sunshield analysts. These polynomials are function of the Sun angles and calculate the SRP

[*]Dr., NASA/Goddard Space Flight Center, University of Maryland Baltimore County, 8000 Greenbelt Road, Greenbelt, MD 20771.

[†]a.i.solutions, Inc. 4500 Forbes Blvd Suit 300, Lanham, MD 20706.

force magnitude and direction in the observatory body frame. All three Sun angles are required to orient the SRP force vector from the body frame into the Earth centered inertial mean J2000 (MJ2K) frame for numerical integrations.

The science orbit is not constrained to a specific type, but a specific size in the Rotating Libration Point (RLP) frame. The freedom in the orbit geometry allows for a wide range of potential science orbits that are suitable for science observations and meet the mission restrictions such as, thermal constraints, tight mass budget, preventing stray light from contaminating the instruments, and meeting communications requirements. The resulting science orbit is highly dependent of the launch epoch and results in a wide variety of different sized halo and quasi-halo orbits.

The goal of this study is to understand how SRP affects the science orbit, focusing on detecting when the constraints on size of the science orbit are violated due to SRP uncertainties. Different types of orbits will be investigated, showing how different attitude profile affect the orbit shape and the maximum/minimum RLP-Y and RLP-Z projections. Moreover, a dynamical explanation to some of the results observed will be provided.

## MISSION TIMELINE AND SCIENCE ORBIT OVERVIEW

JWST will be launched on an Ariane 5 rocket from French Guiana on a direct injection orbit out towards the SEL2 point. Due to the tight mass budget, the mission was designed to place the observatory on the lowest cost transfer trajectory. The science orbit at SEL2 is not constrained to a specific orbit; the requirements are based on a maximum orbit size in the RLP frame, where the $X$-axis of the RLP frame points from the Sun through the Earth–Moon barycenter, the $Z$-axis points to the north ecliptic pole, and the $Y$-axis completes the right-handed system. The requirements are based on a maximum orbit size of $\pm 832,000$ km in the RLP-Y direction and $\pm 520,000$ km in the RLP-Z direction. The science orbit is also required to avoid Earth and Moon shadows. The freedom in allowable orbit geometry allows for a wide range of potential science orbits, maximizing the launch window opportunities. The orbits that do not meet the different constraints are discarded from the launch window analyses.

The injection into the science orbit is broken down into three mid-course correction (MCC) maneuvers designated MCC-1a, MCC-1b, and MCC-2. The three maneuvers are nominally scheduled for execution at launch +12.5 hours, launch +2.5 days and launch +29 days, respectively. All three maneuvers will be planned to ensure that the JWST is captured in the SEL2 regime. The sunshield will be deployed 5 days after launch (i.e. after MCC-1a and MCC-1b have been executed). Due to light sensitivity of the instruments and the thruster configurations, MCC-1a and MCC-1b are planned along the velocity direction and are only able to inject energy into the orbit. To ensure that the observatory does not escape, MCC-1a and MCC-1b will be biased down to 93% of the targeted maneuver to avoid overshoot in the event of an over-performance by the thrusters. On the other hand, MCC-2 acts as the first station-keeping maneuver and will be performed 100%. For more details on the MCC strategy and contingency analysis see Reference 1.

Once JWST has been inserted into a Libration Point Orbit (LPO) around SEL2, routine station-keeping maneuvers are required to keep the observatory from escaping due to the instability of the SEL2 environment combined with the momentum unloads, SRP uncertainties, thruster misalignment and performance error, and orbit determination errors. JWST will be performing station-keeping maneuvers on a 21-day cadence. For both MCC and station-keeping maneuvers, the $\Delta \mathbf{v}$ required for the maneuvers are calculated via a differential correction process in the full ephemeris

model. In order to determine the maneuver size for a specified direction, it is required that at the fourth crossing with the $Y = 0$ plane in the RLP frame the $x$ component of the velocity vector is zero. For a more detailed analysis on how the station-keeping maneuvers for JWST are planned see Reference 2.

The launch window for JWST has been defined by the FDT between 11:30 and 14:00 UTC every day. With the insertion strategy described above, the size and type of orbit to which JWST can be inserted will vary depending on the time of the day and day of the year of the launch. As we can see in Brown et. al paper,[3] the type of orbits JWST could be inserted into range between halo, quasi-halo and Lissajous orbits. However most Lissajous orbits will be discarded from the launch window as they do not meet all the science orbit requirements. These requirements are related to the orbit's size and avoiding shadows by the Earth or Moon.

As an example, Figure 1 shows different orbits JWST can be inserted for different launch times on January 14th, 2021. The black box in each plots corresponds to the boundary of the admissible size for the science orbit in the RLP frame, recall that RLP-Y $\in [-832,000 \quad 832,000]$ km and RLP-Z $\in [-520,000 \quad 520,000]$ km. From now on we will refer to this box as the bounding box. Notice how for January 14th, 2021 only the launches between 12:00 UTC and 13:00 UTC would provide admissible science orbits. Looking at the type of orbits, notice that the arrival LPO launched at 11:30 UTC is a loose quasi-halo orbit. As the daily launch time moves forwards the arrival quasi-halos' become thinner up until 12:10 UTC. From there on the quasi-halo orbits start to grow in size again. Finally, the arrival orbits after 13:20 UTC are Lissajous orbits, some of them violating the limits of the bounding box and presenting possible shadows with the Earth and Moon. This pattern is repeated most of the days through January 2021.

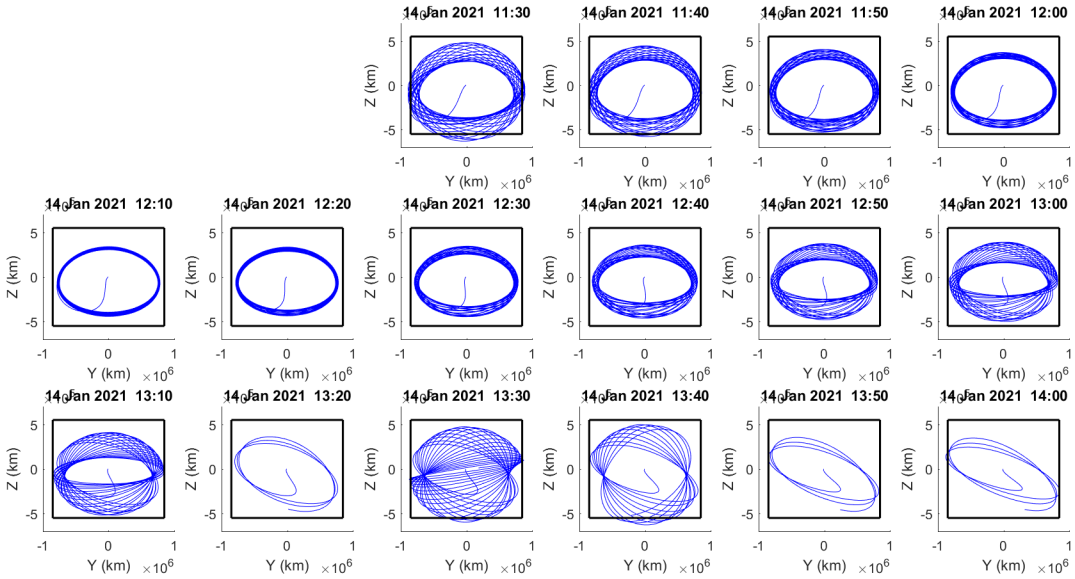


**Figure 1. Arrival orbits at SEL2 for a Launch Window between 11:30 UTC and 14:00 on 14-Jan-2021.**

Another useful way to visually the type of orbit in a launch window is by plotting the intersection of the science orbit with the $Z = 0$ plane in the RLP frame. This type of plot allows us to identify

each orbit with its location on the SEL2 center manifold.[4] Figure 2 shows the intersection of the trajectories presented on the launch window analyses in Figure 1 with the $Z = 0$ plane. Note that launch epoch 13:20, 13:50 and 14:00 did not complete the full 10 year simulation and this is why they look sparse relative to the other orbits.

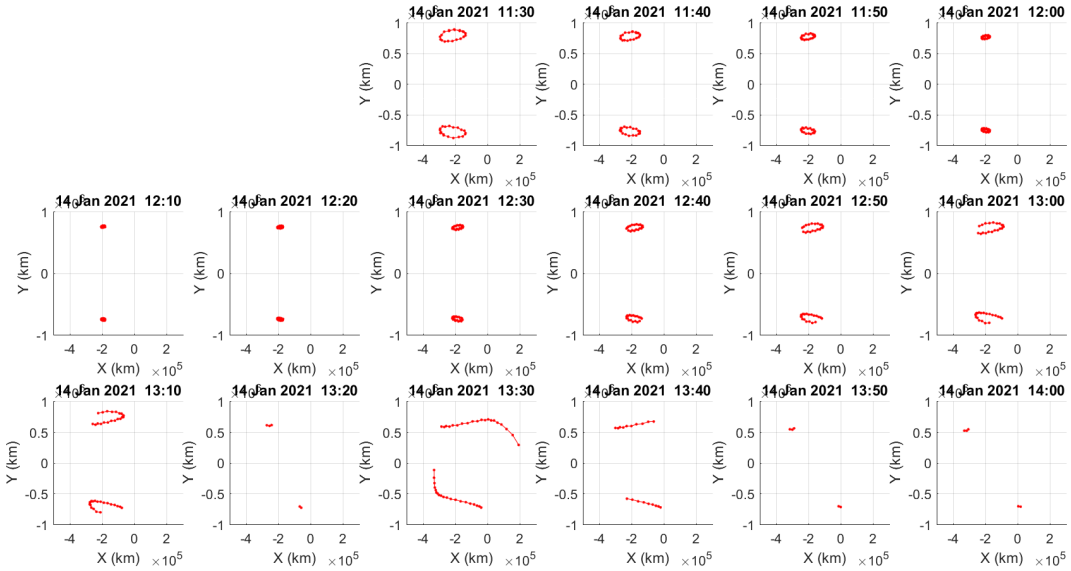


**Figure 2. Projection on the $Z = 0$ plane in the RLP frame of the arrival orbits at SEL2 for the 14-Jan-2021 Launch Window analyses in Figure 1.**

In all these simulations the SRP has been introduced once the sunshield is deployed (i.e. 5 days after launch) using a cannonball model. As we will see in the next section, this model is the simplest and does not account for SRP variations due to changes in the observatory's attitude. The scope of this paper is to analyze how variations on the SRP acceleration during the 10 year mission affect a nominal science orbit, trying to determine how much can these uncertainties affect the size of the science orbit in the RLP-YZ projection, and be able to tell what orbits can end up violating the bounding box.

## SOLAR RADIATION PRESSURE

SRP is the acceleration caused by the exchange in momenta between the solar photons and the satellite's surface. The incident photons will be absorbed or reflected by the surface of the satellite, where the rates of absorption and reflection depend on the reflectivity properties of the surface material. Hence, the total SRP acceleration varies depending on the shape and size of the satellite, its surface materials, and its relative orientation with respect to the Sun-satellite line. Despite being small compared to the gravitational attraction of the main bodies in the system, it is in average at least 2 orders of magnitude larger than the gravitational perturbation of other planetary bodies, and plays an important role in the dynamics of LPO.[5,6]

In the literature we find several ways to model this effect,[7–12] depending on the level of fidelity required. Let us briefly describe the different models and their main differences.

Cannonball model: This is the simplest and most common approach used, where the satellite's

shape is approximated by a sphere.[7] In this case the SRP acceleration ($\mathbf{a_{srp}}$) is always along the Sun-satellite direction, and is expressed as,

$$\mathbf{a_{srp}} = -P_{srp} C_r \frac{A_{sat}}{m_{sat}} \mathbf{r_s}, \tag{1}$$

where $P_{srp} = P_0(R_0/R_{sun})^2$ is the SRP at a distance $R_{sun}$ from the Sun ($P_0 = 4.53 \times 10^{-6}$N and $R_0 = 1$AU), $(A_{sat}/m_{sat})$ is the satellite's area-to-mass ratio, $\mathbf{r_s}$ is the normalized satellite-Sun direction and $C_r \in [1, 2]$ is the reflectivity coefficient. The value of $C_r$ is hard to predict and will depend on the satellite's reflectivity properties. For instance, $C_r = 1$ means that all the sun-light is absorbed, while $C_r = 2$ indicates that all the light is reflected and twice the force is transmitted to the satellite.

Despite its simplicity, this model allows a first estimation on the magnitude of the SRP acceleration and its effects. It is used during the preliminary mission design phase.

N-plate model: This is an intermediate model, where the shape of the satellite is approximated by a collection of flat plates, each of them with different reflectivity properties, representing the different parts of the satellite[7,8] Now the magnitude and direction of the SRP acceleration will vary depending on the satellite's orientation with respect to the Sun-satellite line.

Note that for a flat surface (with area $A$) the total force due to SRP acceleration is the sum of the forces produced by the absorbed photons ($\mathbf{F_a} = P_{srp} A \langle \mathbf{n}, \mathbf{r_s} \rangle \mathbf{r_s}$) and the reflected photons, which can experience specular reflection ($\mathbf{F_s} = 2P_{srp} A \langle \mathbf{n}, \mathbf{r_s} \rangle^2 \mathbf{n}$) and diffusive reflection ($\mathbf{F_d} = P_{srp} A \langle \mathbf{n}, \mathbf{r_s} \rangle (\mathbf{r_s} + \frac{2}{3}\mathbf{n})$). The coefficients $\rho_a, \rho_s$ and $\rho_d$ represent the rates of absorption, specular reflection, and diffusion reflection, which depend on the plates' material properties and satisfy $\rho_a + \rho_s + \rho_d = 1$.

For a satellite defined by a collection of $N$ plates, the total SRP acceleration is given by

$$\mathbf{a_{srp}} = -\frac{P_{srp}}{m_{sat}} \sum_{k=1}^{N} A_k \cos\theta_k \left[ (1 - \rho_s^k)\mathbf{r_s} + 2(\rho_s^k \cos\theta_k + \frac{\rho_d^k}{3})\mathbf{n}_k \right] H(\theta_k), \tag{2}$$

where $A_k$ is the area of each plate, $\mathbf{n}_k$ is the normal vector to the plate and defines its orientation, $\rho_s^k, \rho_d^k$ are its reflectivity properties, and $\cos\theta_k = \langle \mathbf{n}_k, \mathbf{r_s} \rangle$ is the scalar product between $\mathbf{n}_k$ and $\mathbf{r_s}$. The function $H(\theta_k)$ is used to ensure that the side of the plate is accounted for, so $H(\theta_k) = 0$ if $\cos\theta_k < 1$ and 1 elsewhere.

The main advantage of this model with respect to the cannonball model is that it accounts for attitude variations. However, for satellites with a complex shape it can be hard to get an accurate representations with a small amount of flat plates. Moreover, it does not account for the auto-occultation between the plates.

Finite Element: The main limitation on the N-plate model is that auto-occultations between the different plates are not taken into account as it does not have information on the relative position between the plates. To have a high-fidelity approximation, where auto-occultations and secondary reflections from the Sun-light are accounted for, a finite element approximation is necessary.[9,10] Using ray-tracing techniques, it can be determined which parts of the satellite are illuminated and how the light bounces off the surface depending on the different materials and the attitude with respect to $\mathbf{r_s}$.

Unfortunately, this method is very expensive in terms of computational time and it is not advisable to compute the SRP accelerations simultaneously during an orbit propagation. In order to improve

its performance, one should know the attitude profile in advance and compute the SRP acceleration for each attitude, or approximate it using a polynomial fit from intermediate attitudes.[11,12]

### SRP acceleration for JWST

A simple way to describe the SRP acceleration for JWST is in terms of its magnitude $a_{srp} = ||\mathbf{a_{srp}}||$ and the offset angle $\theta$ (i.e. angle between $\mathbf{a_{srp}}$ and $\mathbf{r_s}$). This allows us to compare the high-fidelity approximation with the cannonball model, where $a_{srp}$ is constant and $\theta$ is zero.

To model the unique SRP force for JWST at a high-fidelity the FDT uses a polynomial curve fit provided by the sunshield analysts. The polynomials are a function of Sun-pitch and Sun-roll that calculate the SRP force magnitude and direction in the observatory body frame. To orient the SRP force in the MJ2K frame required for numerical integration, all three Sun angles are required to orient the SRP force from the body frame into the MJ2K frame. Unlike the cannonball model, the SRP force for JWST is not aligned along the Sun-to-Observatory vector.

The angles Sun-pitch, Sun-roll, and Sun-yaw define the attitude of JWST with respect to the Sun-observatory line. A visual definition of these angles can be found in Figure 3*. To protect the observatory from external sources of light and heat, the sunshield must always be between the Sun/Earth/Moon and the observatory, which limits JWST's attitudes. Due to the shape and location of the sunshield, the allowed Sun angles range between $-53°$ to $0°$ for Sun-pitch, $\pm 5°$ for Sun-roll, and $\pm 180°$ for Sun-yaw.

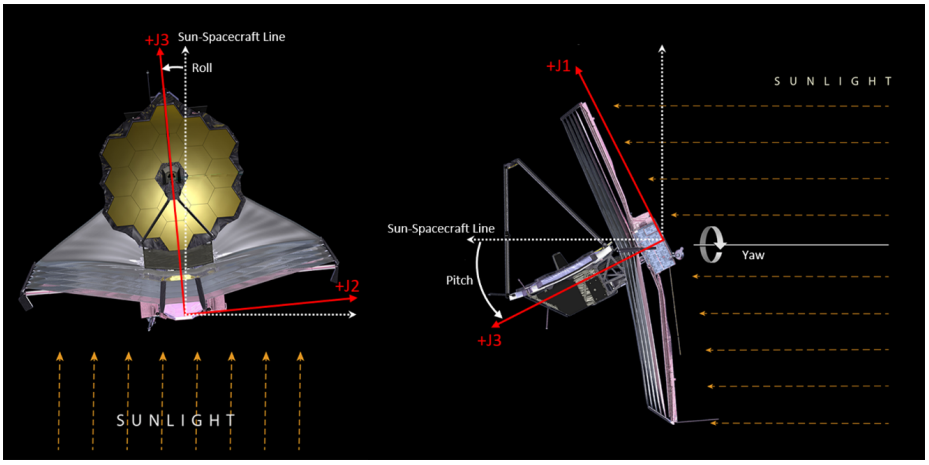


**Figure 3. Sun angle definitions for JWST.**

Figure 4 presents JWST high-fidelity SRP acceleration approximation for different Sun-pitch and Sun-roll angles. The left plot shows the variation of $a_{srp}$ and the right plot the variation of the offset angle with respect to these two Sun angles. We can see that $a_{srp}$ experiences variations between $2.05 \times 10^{-10}$ and $1.15 \times 10^{-10}$ km/s$^2$, and the offset angle $\theta$ can be up to $24°$. Note that for a fixed Sun-pitch and Sun-roll, varying Sun-yaw does not affect the affect the SRP acceleration magnitude or the offset angle, just the relative position between the two vectors varies. As Sun-yaw varies between $180°$ to $-180°$, $\mathbf{a_{srp}}$ describes a cone centered along the Sun-observatory line with a cone angle of $\theta$.

*Image credit: `https://jwst-docs.stsci.edu/display/JTI/JWST+Observatory+Coordinate+System+and+Field+of+Regard` [Accessed 27 June 2019]

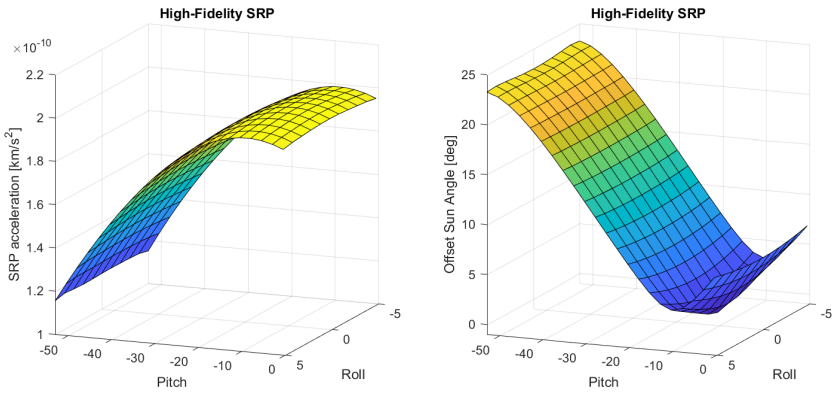


**Figure 4. SRP acceleration for JWST using polynomial fit. Variation of SRP with respect to Sun-pitch and Sun-roll. Left: SRP acceleration magnitude. Right: SRP offset angle with respect to the Sun-to-observatory vector.**

Given that JWST has an estimated area-to-mass ration of 0.025515 $m^2$/kg, $P_{srp}$ at the SEL2 vicinity (1.01 AU) is $4.47995 \times 10^{-6}$ and as the sunshield is highly reflective an estimated $C_r = 1.8$ is considered. Using the cannonball model in Eq. 1, the estimated SRP acceleration is $2.0575 \times 10^{-10}$ km/$s^2$, which is close to the maximum $a_{srp}$ in Figure 4.

Instead of the cannonball model we now consider a 1-plate approximation, with $A = 161\ m^2$, $\mathbf{n} = (0.9848, 0.000, -0.1736)$ (tilted $10^\circ$ with respect to the ecliptic plane) and reflectivity coefficients $\rho_s = 0.8, \rho_d = 0$. Figure 5 shows the SRP acceleration profile for this 1-plate approximation (Eq. 2), which is similar to the high-fidelity approximation in Figure 4. The major differences between the two models is seen with the offset angle. Adding more plates and small changes to the reflectivity coefficients could produce better agreement between the two models, however this not the scope of this paper.

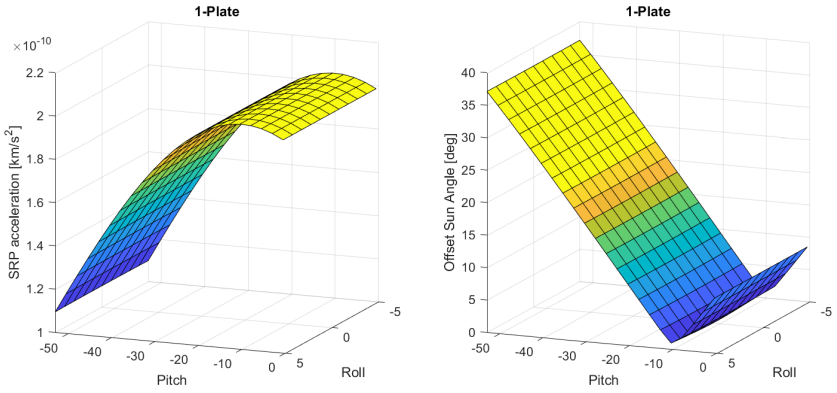


**Figure 5. SRP acceleration for JWST using 1-plate model. Variation of SRP with respect to Sun-pitch and Sun-roll. Left: SRP acceleration magnitude. Right: SRP offset angle with respect to the Sun-to-observatory vector.**

## SRP EFFECT ON LIBRATION POINT ORBITS

To describe how SRP affects the motion of JWST in the SEL2 vicinity we use the classical Circular Restricted Three Body Problem (CRTBP) with Sun and the Earth/Moon as primaries and including the SRP acceleration. Recall that the CRTBP assumes that Sun and the Earth/Moon barycenter are point masses moving around their common center of mass in a circular motion due to their mutual gravitational attraction. The spacecraft is a mass-less particle that does not affect the motion of the two primaries but is affected by the gravitational attraction of the two primaries as well as the SRP.

It is common to consider a rotating reference frame with the origin at the center of mass of the Sun-Earth/Moon system, where Sun and Earth/Moon barycenter are fixed on the $x$-axis (with the positive side pointing towards the Earth/Moon barycenter), the $z$-axis is perpendicular to the ecliptic plane, and the $y$-axis completes an orthogonal positive oriented reference system. The units of mass, distance, and time are normalized so the total mass of the system is 1, the Earth - Sun distance is 1, and the period of one Earth - Sun revolution is $2\pi$. With these assumptions, the equations of motion are given by

$$\ddot{x} - 2\dot{y} = \frac{\partial \Omega}{\partial x} + a_x, \qquad \ddot{y} + 2\dot{x} = \frac{\partial \Omega}{\partial y} + a_y, \qquad \ddot{z} = \frac{\partial \Omega}{\partial z} + a_z, \tag{3}$$

where $\Omega(x, y, z) = \frac{1}{2}(x^2 + y^2) + \frac{1-\mu}{r_{ps}} + \frac{\mu}{r_{pe}}$, with $r_{ps} = \sqrt{(x+\mu)^2 + y^2 + z^2}$ and $r_{pe} = \sqrt{(x+\mu-1)^2 + y^2 + z^2}$ the Sun-satellite and Earth/Moon barycenter-satellite distances respectively, and $\mathbf{a_{srp}} = (a_x, a_y, a_z)$ is the SRP acceleration.

For simplicity, in this section the SRP acceleration of JWST is approximated by the 1-plate model presented in the previous section. Notice that $P_{srp}$ depends on the inverse of the Sun-spacecraft distance in the same way as the Sun's gravitational attraction. It is common to define the parameter $q_{srp}$ as the ratio between the SRP acceleration ($P_{srp}A_{sat}/m_{sat}$) and the acceleration due to the Sun's gravity ($Gm_s/r_{ps}$). With this, Eq. 2 for 1-plate can be rewritten as

$$\mathbf{a_{srp}} \;=\; -q_{srp}\frac{1-\mu}{r_{ps}^2}\cos\theta\left[(1-\rho_s)\mathbf{r_s} + 2(\rho_s\cos\theta + \frac{\rho_d}{3})\mathbf{n}\right], \tag{4}$$

where $q_{srp} = K_s(A_{sat}/m_{sat})$ for $K_s = (P_0 R_0^2/GM_{sun}) = 7.7065 \times 10^{-4}$ when $A_{sat}$ and $m_{sat}$ are given in $\mathrm{m}^2$ and kg, respectively.

Recall that JWST has an estimated area-to-mass ratio of 0.0255 $\mathrm{m}^2$/kg, hence $q_{srp} = 1.9652 \times 10^{-6}$. Note that $q_{srp}$ is equivalent as the lightness number ($\beta$) for a solar sail, which measures its efficiency.[6] Current solar sail technology considers sail lightness numbers close to $0.002$, hence JWST can be seen as a very inefficient solar sail.

Let us now describe how the extra effect of $\mathbf{a_{srp}}$ affects the dynamics around SEL2 and the associated LPOs. It is well know that when $\mathbf{n}||\mathbf{r_s}$ all five equilibrium points $L_{1,\ldots,5}$ are displaced towards the Sun.[5,6] By tilting the plate's attitude, i.e. changes in $\mathbf{n} = (n_x, n_y, n_z)$, the equilibrium points can be artificially displaced above and below the ecliptic plane if $n_z \neq 0$ and away from the Sun-Earth/Moon barycenter line if $n_x \neq 0$. The different equilibrium points for the different fixed attitudes are displace around a sphere-shaped object where $L_i$ is the point in the surface that is further away from the Sun. How much these equilibrium points are displaced depends on $q_{srp}$ magnitude. For the case of JWST we have estimated a maximum displacement along the Sun-Earth

line $\approx$ 582 km, a maximum displacement away from the Sun-Earth line in the ecliptic plane of $\approx$ 682 km, and a maximum displacement above the ecliptic plane of $\approx$ 508 km.

A similar effect is observed when we look at the LPOs around SEL1 and SEL2.[6] As with the equilibrium points, if the attitude is fixed along the Sun-satellite line ($\mathbf{n}||\mathbf{r_s}$), the halo, quasi-halo, and Lissajous orbits are displaced towards the Sun. When the attitude is fixed but with a certain offset angle with respect to $\mathbf{r_s}$ then all these LPOs are displaced accordingly, with the same behavior as the artificial equilibria. Hence, we can say that the qualitative behavior around the displaced equilibria is almost the same as for the SEL2.[5,6]

Finally, notice that the discussion above is true if the flat-plate attitude is kept fixed with respect to the Sun-satellite line, which does not reflect the reality of JWST as its attitude will vary as it moves along a LPOs. Note that when the attitude changes, the set of LPOs are displaced, as well as their stable and unstable manifolds. Hence for each attitude change, the relative position of JWST with respect to the unstable manifolds will change. One can think of these phenomena as changing the phase space each time the attitude changes. How these changes affect JWST trajectory is hard to determine, as the attitude profile is unknown and will depend on JWST observations. However, these changes will affect the escape rate as well as the $\Delta\mathbf{v}$'s for station-keeping. In the next section we focus on some of these changes for a full ephemeris model.

## EFFECT OF SRP ON JWST ORBIT SHAPE

As we have seen in the first section, the resulting science orbit is tightly coupled to the launch epoch. The left plot on Figure 6 shows four different type of orbits for JWST following the three MCC maneuver strategy described previously, each with a different launch times on January 14th, 2021. Three of the four are quasi-halo orbits (with different sizes) and one of them is a Lissajous orbit *. The right hand side of Figure 6 displays the intersection of the science orbit with the $Z = 0$ plane. There we can easily identify each type of orbit and their relative location on the center manifold. The points that rotate around the $(-2 \times 10^5, \pm 0.8 \times 10^5)$ point correspond to quasi-halo orbits. In this projection, the wider the orbit is, the more loose the quasi-halo will be. On the other hand, the points that rotate around the center $(0, 0)$ correspond to a Lissajous orbit.

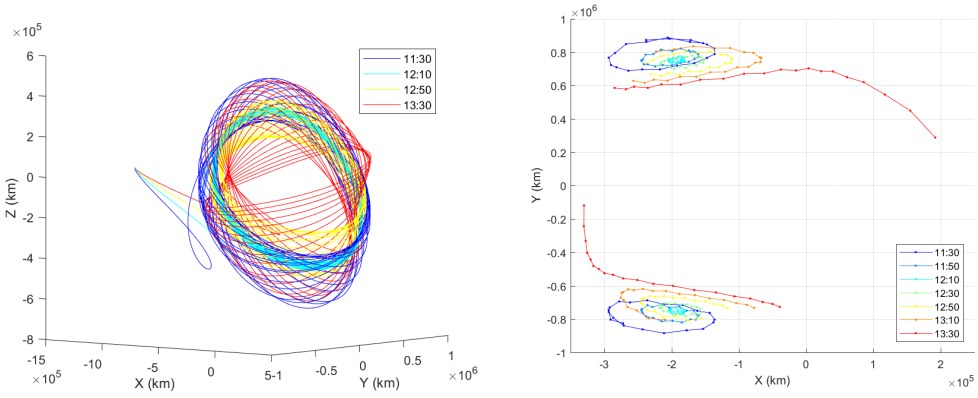


**Figure 6. Left: Possible science orbits for JWST for different launch opportunities on 14-Jan-2021. Right: Intersection of the science orbit with the $Z = 0$ RLP plane.**

*Most Lissajous orbits would be rejected from the launch window due to the requirement of avoiding the Earth and Moon shadows.

As already mentioned, the main goal of this study is to determine how variations on SRP acceleration, due to changes on JWST's attitude during the mission lifetime, affect the size of the orbit paying special attention to the violation of the bounding box in the RLP reference frame. To address this problem, several analyses have been performed. First, we study the variation of the orbit size when the attitude is kept fixed during the whole mission. The idea was to see if in the full ephemeris model the libration point orbits are also displaced from nominal reference orbit as it happens in the CRTBP. Second, several simulations with random attitude variations have been performed to see how this impacts the orbit shape and size.

For this study three different orbits have been selected, all of them belonging to the 14-Jan-2021 launch window. In particular these orbits correspond to the launch time 11:50 UTC (`orb01`), 12:10 UTC (`orb02`) and 12:50 UTC (`orb03`), which are displayed in Figure 7 from left to right respectively. Mention that although `orb01` violates the bounding box, it is also interesting to analyses how SRP affects its orbit. For the record, all of these orbits have been computed using the cannonball model for SRP and serve as reference.

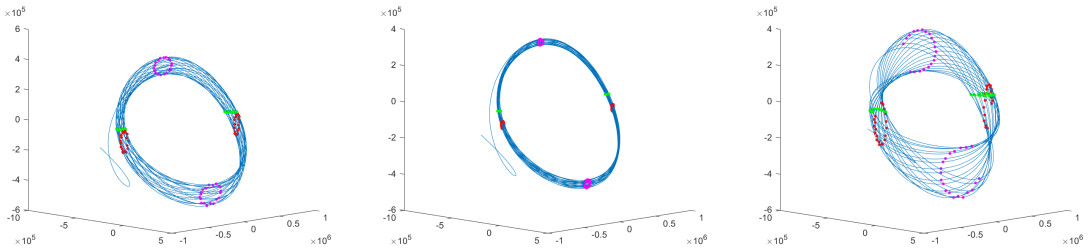

**Figure 7. Reference orbits for the SRP analysis. From left to right 11:50 UTC, 12:10 UTC and 12:50 UTC launch on 14-Jan-2021. Green points are the intersection of the orbit with the $Z = 0$ RLP plane; Red points are the max and min in the RLP-Y at each revolution; Magenta points are the max and min in the RLP-Z at each revolution.**

For each of the orbits in Figure 7 distinctive points on the orbit are highlighted: the location of the intersection of the orbits with $Z = 0$ in the RLP plane (green points) and the location of the maximum and minimum RLP-Y and RLP-Z projection (red and magenta points respectively) per orbital period. These characteristics will help describe the orbital variations in shape and size.

### SRP effects for a fixed attitude

Let us start by focusing on how keeping constant fixed attitude throughout the full mission affects the shape of the orbit. Recall that JWST's attitude is defined in terms of the allowed Sun angles. From now on, we call Sun-Neutral the attitude for which the SRP acceleration is aligned with the Sun-observatory line. From Figure 4 we can see that Sun-Neutral corresponds to a Sun-pitch of $-10.05°$, Sun-roll of $0°$, and Sun-yaw free. Note that keeping a fixed Sun-Neutral attitude is equivalent to using the cannonball model for the SRP.

For the three launch window opportunities dates presented above, we have performed a full 10 year simulation, including the SRP after the sunshield deployment and keeping the attitude fixed for the full orbit propagation. We have scanned different attitudes, varying Sun-pitch between -50 and 0 degrees with steps of 10 degrees, varying Sun-yaw between -180 and 180 degrees with steps of 30 degrees and keeping Sun-roll to 0 degrees.

The intersection of all of these orbits with the $Z = 0$ plane is presented in Figure 8. The black

curve corresponds to the orbit with a Sun-Neutral attitude, which is used as reference. As we can see the overall shape of the orbit is the same for the different fixed attitudes. The displacement between the orbits is hard to see due to the scaling factors. Figure 9 is a zoom close to different points on the $Z = 0$ intersection for `orb02`, where we can appreciate the displacement of the different orbits. The color is used to identify the same Sun-yaw values trajectories. Notice how at the different intersection points the same structure is preserved, presenting a cone of possible locations. The size of these cone is kept more or less constant in most of the cases. In some cases the distance between the points in the cone can grow, this is mainly due to changes in the phase of the orbit if we look at `orb01` and `orb02`. The case for `orb03` is slightly different as this quasi-halo orbit is close to the boundary between the quasi-halo and Lissajous orbits (see Figure 6). It is know that the boundary between these two type of orbits is the unstable manifold of the planar Lyapunov orbit. Being so close to an unstable manifold can make the trajectories experience more instability deriving on larger displacement between nearby trajectories.

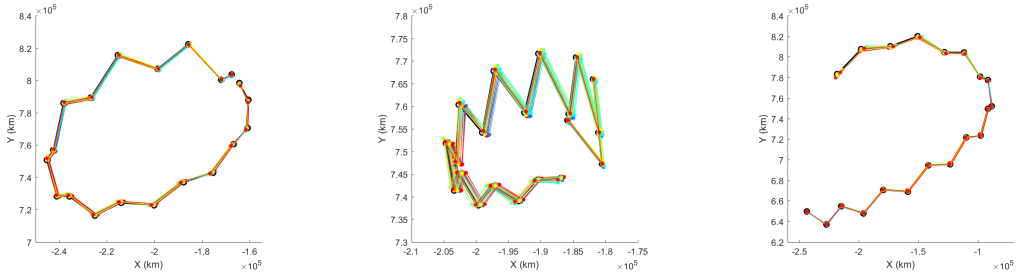


**Figure 8. Intersection on the $Z = 0$ RLP plane for the orbits scanned for different attitudes. From left to right `orb01`, `orb02` and `orb03`. The black curve corresponds to Sun-Neutral.**

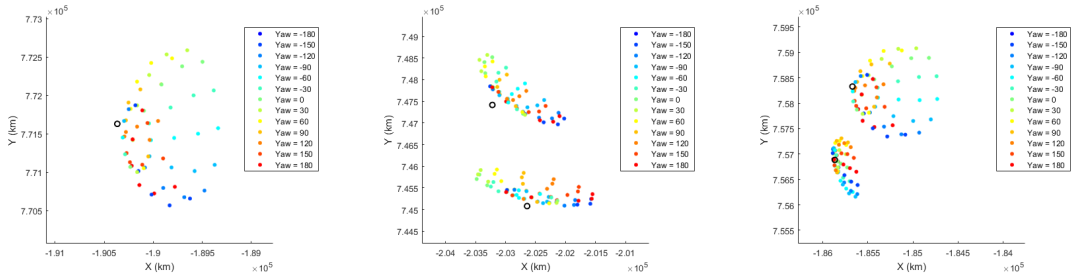


**Figure 9. Simulations for `orb01` and different fixed attitudes, intersection with the $Z = 0$ plane. Zoom around the different intersection points. The color of each point corresponds to the same Sun-yaw angle.**

For each of the trajectories, the maximum and minimum RLP-Y and RLP-Z at each orbital period has been computed. These values are indicatives of the trajectory's distance to the bounding box and the growth of the orbit. Figure 10 shows the difference between the maximum RLP-Y and RLP-Z for the Sun-Neutral trajectory and the fixed attitude trajectory (similar results are observed with the minimum RLP-Y and RLP-Z distances to Sun-Neutral). The top plots show the RLP-Y difference and the bottom plots show the RLP-Z difference. As in Figure 9 each color represents a fixed Sun-yaw angle. It can be seen that for all three trajectories, the distance to Sun-Neutral oscillates, but the differences are consistent with each Sun-yaw value, having a collection of orbits one above the other. For `orb01` these distances flip, this is probably due to a change in the quasi-halo orbit

phasing angle as this is a loose quasi-halo orbit. Moreover, notice how for `orb01` and `orb02` (left and center plots) the distances oscillate, but never experience a drastic drift as it happens on `orb03` towards the end of the simulation. This drastic change might be related to the proximity to the planar Lyapunov unstable manifold. Notice how for the other two orbits, the RLP-Y maximum displacement oscillates but is always below the 3000 km and the RLP-Z maximum displacement is always below 5000 km.

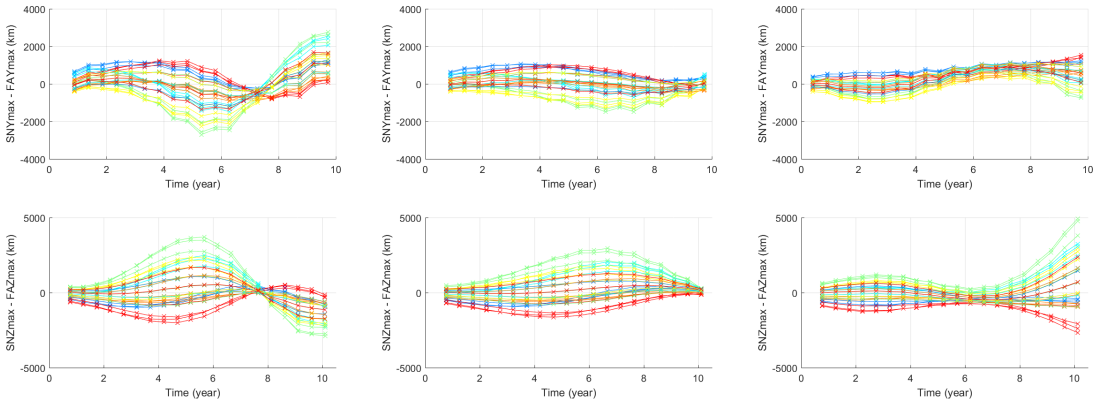


**Figure 10. Difference between maximum RLP-Y (top) and RLP-Z (bottom) of the Sun Neutral trajectory and the fixed attitude trajectory. From left to right launch epoch related to `orb01`, `orb02` and `orb03` respectively.**

The results show that if the reference science orbit is not close to the boundary between Lissajous and quasi-halo orbits, keeping a fixed attitude essentially displaced the reference orbit. This is not true when the orbit is close to the boundary between these two type of orbits as we are close to an unstable manifold and the behavior is hard to predict.

### SRP effects for a variable attitude

Let us now analyze the effect of changing the attitude through a 10 year simulation for the three different launch opportunities. Currently there is no Design Reference Mission (DRM) for the objects in the sky that will be observed, hence we do not have a predefined attitude profile for JWST. A 14-day predicted attitude schedule will be provided to the FDT on a weekly basis once JWST is in its science orbit. The only information available for long-term propagation beyond the available 14-day attitude schedule is the limitations on the Sun-pitch and Sun-roll between -53° and 0° and $\pm 5°$, respectively. For this reason we have performed simulations with a different set of randomly distributed attitude profiles and study what type of behaviors appear.

We have defined four different type of attitude schedules in an attempt to capture a variety of scenarios, including a worst case scenario. Here we present the results for the four different attitude schedules with 10-year simulations generated for each different attitudes schedule for a total of 40 long-term simulations. For each of the cases, the set of Sun-pitch, Sun-roll and Sun-yaw angles are chosen randomly following a uniform distribution within the admissible set of attitudes. The four different attitude schedules are: Case 1, the attitude changes every 7 days; Case 2, the attitude changes every 21 days; Case 3, the attitude changes alternating every 3, 15, 9, 6 and 18 days in a loop; Case 4, the time between attitude changes is chosen randomly between 1, 2, 3, ..., 20 to 21 days. This last case is the most realistic as JWST will be observing different parts of the sky

in between the 21-day station-keeping cadence. In total we have 40 different attitude profiles and associated trajectories to analyze for each launch opportunity.

Here we do not show the results of the trajectories on the $Z = 0$ plane, as it is hard to identify patterns in this projection as the motion is chaotic around the Sun-Neutral trajectory. The results show that for all three launch opportunities the shape of the orbit is preserved and no drastic deviation from the Sun-Neutral intersections are observed. We do observe larger deviations from Sun-Neutral in the case of attitude changes every 21 days.

Figures 11, 12 and 13 show the difference between the maximum and minimum RLP-Y (top) and RLP-Z (bottom) displacement of the random attitude profile trajectory and the Sun-Neutral trajectory. In each plot the simulations are grouped by the different attitude schedules, from left to right cases 1 to 4.

In all three cases, we can appreciate that the trajectories that experience larger variations on the distances are the simulations where the attitude is changed every 21 days. This is due to long exposure to large pitch angles, where the offset angle between the Sun-line and the SRP acceleration is the largest. We also observe that variations in the RLP-Z direction are in general larger than those in the RLP-Y direction. The first ones are bounded by 5000 km in most of the cases, while the RLP-Y is always below 4000 km. Only a few trajectories fall out of these bounds, and the specific cases must be studied to understand what produced this long drift in one of the directions.

We also note that again we see that `orb03` presents a more unstable behavior than `orb01` and `orb02`, especially in the RLP-Z direction. As it happened when we were analyzing the results for a fixed attitude, the proximity of these trajectories with planar Lyapunov unstable manifold might play a role.

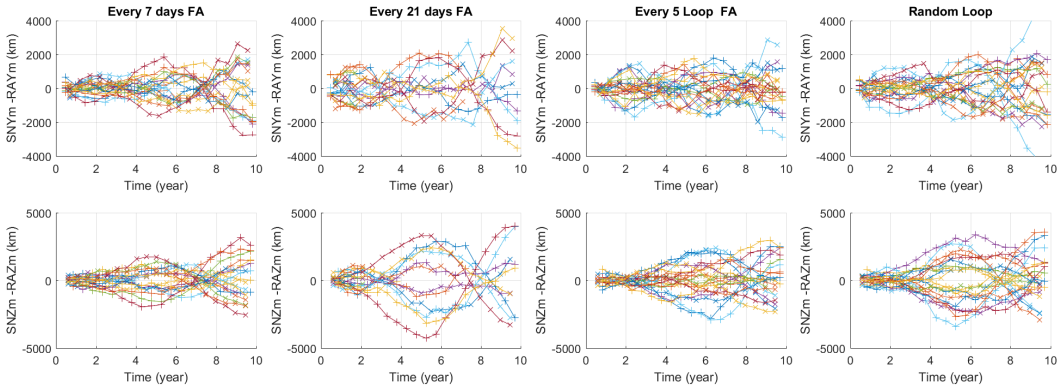


**Figure 11. For `orb01` difference between the maximum and minimum RLP-Y (top) and RLP-Z (bottom) of the Sun-Neutral trajectory and the random attitude profile. From left to right attitude schedule of case 1, 2, 3 and 4 respectively.**

## CONCLUSION

In this paper we have studied the effects on JWST's science orbit due to the variations of the SRP acceleration due to changes on its attitude during the mission lifetime. As test cases, three different quasi-halo orbits have been chosen, a tight quasi-halo and two loose quasi-halo orbits, one of them very close to the boundary between the quasi-halo and Lissajous orbits.

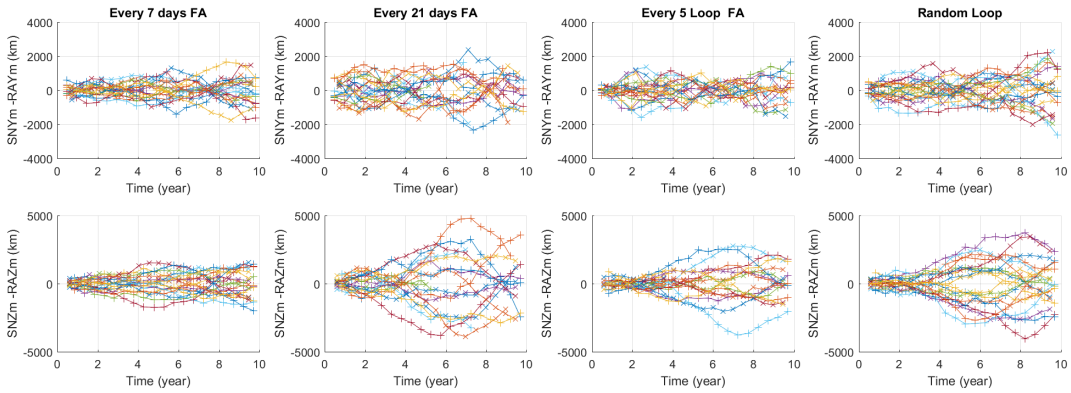


**Figure 12. For `orb02` difference between the maximum and minimum RLP-Y (top) and RLP-Z (bottom) of the Sun-Neutral trajectory and the random attitude profile. From left to right attitude schedule of case 1, 2, 3 and 4 respectively.**

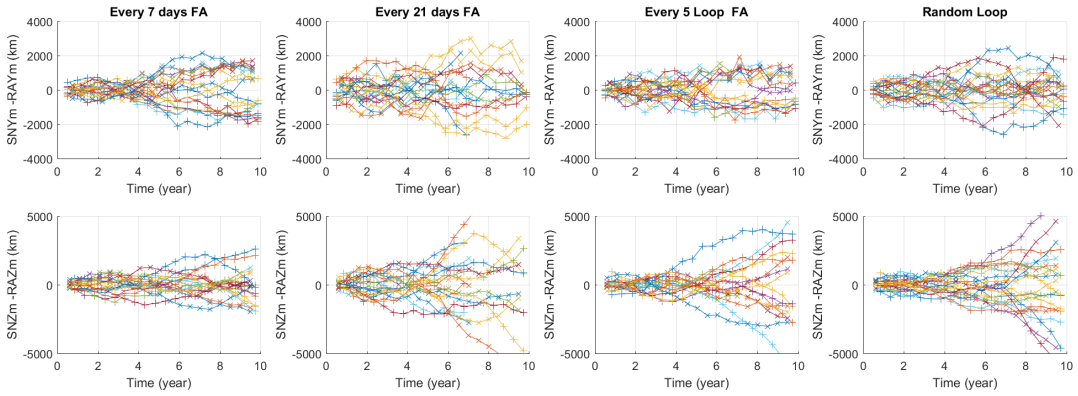


**Figure 13. For `orb03` difference between the maximum and minimum RLP-Y (top) and RLP-Z (bottom) of the Sun-Neutral trajectory and the random attitude profile. From left to right attitude schedule of case 1, 2, 3 and 4 respectively.**

From the results in the simulations we have seen that in most of the cases the variations in the RLP-Y distance are always below 4000 km, while the distances in the RLP-Z direction can vary up to 5000 km. Further investigations with a larger sample of orbits should be investigated. However this allows us to redefine the bounding box by reducing the RLP-Y and RLP-Z accordingly to ensure that the trajectories do not violate the original bounding box.

The results also show that the quasi-halo orbits close to the boundary with the Lissajous orbits are more sensitive to changes on the attitude than the other orbits. We might also want to take these orbits away from the launch window analysis to avoid large variation on the orbit as the attitude changes.

## ACKNOWLEDGMENT

This work has been funded by the JWST project under the Goddard Planetary and Heliophysics Institute Task 595.001 in collaboration with the University of Maryland Baltimore County (UMBC) under NNG11PL02A.

## REFERENCES


[1] T. Rashied, B. Stringer, and J. Petersen, "Mid-Course Correction Contengency Analysis for James Webb Space Telescope (AAS 19-816)," *2019 AAS/AIAA Astrodynamics Specialist Conference*, August 2019.

[2] J. Petersen, "L2 Station Keeping Maneuver strategy for the James Webb Space Telescope (AAS 19-806)," *2019 AAS/AIAA Astrodynamics Specialist Conference*, August 2019.

[3] J. Brown, J. Petersen, B. Villac, and W. Yu, "Seasonal Variations of the James Webb Space Telescope Orbital Dynamics (AAS 15-802)," *2015 AIAA/AAS Astrodynamics Specialist Conference*, August 2015.

[4] A. Jorba and J. Masdemont, "Dynamics in the center manifold of the collinear points of the restricted three body problem," *Physica D*, Vol. 132, 1999, pp. 189–213.

[5] A. Farres and A. Jorba, "Periodic and Quasi-Periodic Motion of a Solar Sail close to SL1 in the Earth-Sun System," *Celestial Mechanics and Dynamical Astronomy*, Vol. 107, June 2010, pp. 233–253.

[6] A. Farres, "Catalogue on the Dynamics of a Solar Sail around L1 and L2," *Proceedings of the 4th International Symposium on Solar Sailing*, January 2017.

[7] D. Vallado, *Fundamentals of astrodynamics and applications*. New York, Springer, 1997.

[8] J. A. Marshall and S. B. Luthcke, "Modeling radiation forces acting on Topex/Poseidon for precision orbit determination," *Journal of Spacecraft and Rockets*, Vol. 31, No. 1, 1994, pp. 99–105.

[9] M. Ziebart, *High precision analytical solar radiation pressure modelling for GNSS spacecraft*. PhD thesis, University of East London, 2001.

[10] M. Ziebart, "Generalized Analytical Solar Radiation Pressure Modeling Algorithm for Spacecraft of Complex Shape," *Journal of Spacecraft and Rockets*, Vol. 41, No. 5, 2004.

[11] J. W. McMahon and D. J. Scheeres, "New Solar Radiation Pressure Force Model for Navigation," *Journal of Guidance, Control and Dynamics*, Vol. 33, 2010, pp. 1418–1429, 10.2514/1.48434.

[12] A. Farres, D. Folta, and W. C., "Using Spherical Harmonics to model Solar Radiation Pressure Accelerations," *AAS/AIAA Astrodynamics Specialist Conference*, August 2017.